

## Chemical reaction and viscous dissipation effect on MHD oscillatory blood flow in tapered asymmetric channel

Sasikumar J., Senthamarai R.\*

*Department of Mathematics, College of Engineering and Technology,  
SRM Institute of Science and Technology, Kattankulathur-603 203,  
Chengalpattu District, Tamilnadu, India*

*\*Corresponding author: senthamr@srmist.edu.in*

(Received 31 March 2022; Revised 7 September 2022; Accepted 8 October 2022)

MHD viscous oscillating type blood flow through lumen in arteries and varicose veins motivating to the study of blood flow in disordered blood vessels and veins. The blood flow in disordered nervous system, like varicose veins and other micro arteries in respiratory system is modeled geometrically in the shape of tapered curvy walls of varying cross section which is the new approach in this problem and the same has advantage compared to the other geometrical channel shapes. Blood taken as viscoelastic and optically thick fluid flowing through porous structure. Magnetic force considered in normal direction to the nervous system. Viscous dissipation and chemical reaction effects on blood flow are analyzed.

**Keywords:** *blood flow, optically thick fluid, chemical reaction and viscous dissipation.*

**2010 MSC:** 58D30, 76Zxx, 93C20, 93A30

**DOI:** 10.23939/mmc2022.04.999

### 1. Introduction

Blood flow or hemodynamic problems played a vital role in medical biology and physiopathology. Blood is mixed with many substances like nutrients, oxygen, carbondioxide, proteins, minerals etc. and composed of plasma with water and glucose. Blood circulation performs different types of function, transports unwanted metabolic particles. In fluid flow analysis, in earlier days, the blood had been considered as vital fluid. Later, since the plasma in blood acts as a Newtonian fluid and it exerts shear thinning behaviour in haematocrit and it is necessary to consider it as non Newtonian fluids. Blood portrays laminar characteristics, its velocity is high in the center of the channel and comparatively low near walls. Various studies about blood flow include measuring velocity of the blood in many different circumstances. Authors those who are interested in blood flow analysis studied with various geometrical aspects, convections and with different category of fluids.

Ramachandra Rao et al. [1] discussed MHD oscillatory flow of blood in which blood has been considered as Newtonian, homogeneous viscous fluid. He studied its unsteadiness while the fluid flows through the channels of unsteady cross sections. These flows reveal a constant streaming component corresponds to non-linear equations governing the motion. Ogulu et al. [2] analyzed the blood flow characteristics in a cardio vascular system with diseased artery and the effects of heat transfer. The results are further analyzed and compared with blood characteristics.

Norsarahaida et al. [3] studied magneto-hydrodynamic flow of blood as an electrically conducting fluid which flows in axis symmetric through an irregular multi stenosis arteries. The governing equations have been solved by marker and cell and over-relaxation methods. The inference of the results has significant clinical implications. Hatami et al. [4] analyzed the heat transfer effect of blood flow, where blood is considered as non-Newtonian nano fluid moves in a porous medium subject to magnetic field. The governing equations are solved using 4th order RK method and concluded that the velocity

is decreased, the concentration of nano particles and the temperature increased with the increase of MHD parameters.

Shit et al. [5] studied blood flow while the transfer of heat which flows through an over lapping constricted artery. Here it has been considered as Newtonian fluid and assumed the viscosity depending on temperature and tried to match with the original biological system. Adhikary et al. [6] studied oscillatory magneto-hydrodynamic flow of blood through which the arteriole has been considered as porous medium. The effect of heat and mass transfer has been investigated with the influence of chemical and magnetic fields.

Ali Abbas et al. [7] combined the blood flow effects of slip and MHD, peristaltic in nature with varying porous medium which resembles the nature of blood flow in a diseased blood vessel and to study critical real situations.

Pooria et al. [8] has studied the pulsatile laminar flow of MHD in a porous arteries where the blood is considered as non-Newtonian fluid which is incompressible. The acceleration of the body and the pressure gradient are periodically influenced by this flow has been studied numerically. Misra et al. [9] presented a study of the unsteadiness in blood flow with temperature change in permeable vessel subject to magnetic field and the impact of thermal slip due to varying heat source with respect to velocity slip near the wall which resembled with the real time situations. Mirza et al. [10] studied the electro magneto-hydrodynamic approach for the blood flow with suspensions occurred by the particles through the vessel involved in surgery which accompanies in getting relieved from pains and solved for the dimensionless velocity of blood and its particles by using Hankel transforms. Kai-Long Hsiao et al. [11] studied the MHD effect and the energy management of applied thermal system influenced by the magnetic field and the viscous dissipation. The micropolar and nano fluids are combined together and the 2D flow of incompressible fluid has been considered in a semi-infinite stretching plate and effect of change with heat and mass transfer has been derived.

Sreeparna and Shit [12] extended their work [5] to the fluid flow through arteries with stenotic conditions, blood is the fluid considered as Newtonian fluid, assumed rigid wall (arteries), viscous dissipation and the effect of heat transfer in such situation has been analyzed. The governing equations have been solved by FEM and Alternating Direction Implicit scheme. Davar Ali et al. [13] studied the computational fluid dynamics analysis with bone tissue cells by developing its common structure and porosity levels and compared the results to analyze the permeability.

Building-up of plaque narrows arteries, decreasing blood flow to the heart, causing chest pain, shortness of breath, or other coronary artery disease signs and symptoms. Recently, by Implementing Navier–Stokes equations in a cylindrical coordinate system and assuming axial symmetry under laminar flow conditions, Kafle et al. [14] analyzed the blood flow through curved artery with mild stenosis. Also Sasikumar et al. [15] discussed the heat and mass transfer effects on MHD Oscillatory flow of a couple stress fluid in an asymmetric tapered channel. In this paper, it is analyzed about the effects of heat and mass transfer effects on oscillatory flow of an incompressible electrically conducting viscous fluid under the influence of couple stress force in an asymmetric channel filled with porous medium.

The analysis made and reviewed about various environments of blood flow analysis by numerous authors, it has been decided to consider the viscous dissipation effect in blood flow analysis, the flow of the fluid is oscillatory and the channel in which the fluid flows is tapered asymmetric. As the governing equations are non-linear, it has been used homotopy perturbation method which is proved to be faster convergence towards the accurate solution [16,17]. Hence its most reliable method for solving problems on nonlinear coupled equations which is widely encountered in fluid dynamics research area to solve it and results discussed. This problem has not been discussed earlier using HPM method by any other author.

### 2. Nomenclature

#### Dimensional Variables

$C^*$	Concentration
$C_P$	Specific heat at constant pressure
$C_0^*, C_1^*$	Concentration at the walls
$D$	Mass diffusion
$T^*$	Temperature
$T_0^*, T_1^*$	Wall temperatures
$k^*$	porous medium permeability coefficient
$k$	Thermal conductivity
$K_r^*$	Chemical reaction parameter
$p^*$	Dimensional pressure
$q^*$	Dimensional radiative transfer
$t^*$	Dimensional time
$u^*$	Axial velocity

#### Greek symbols

$\alpha$	Viscosity ratio
$\beta_0$	Viscoelastic or secondgrade parameter
$\beta_1$	Thermal expansion coefficient
$\beta_2$	Coefficient of mass expansion
$\sigma_e$	Conductivity of the fluid
$\gamma$	Mass diffusion ratio
$\varepsilon$	Periodic parameter coefficient
$\theta$	Dimensionless temperature
$\mu$	Dimensionless wave number
$\nu$	Viscosity of fluid kinematic viscosity
$\rho$	Fluid density
$\varphi$	Dimensionless concentration
$\psi$	Phase, angle
$\omega$	Frequency of oscillation
$\omega t$	Periodic frequency parameter

#### Non dimensional variables

$a_1, a_2$	amplitudes of the wavy walls
$d$	Average channel width
$D$	Mean half width of the channel
$Ge$	Modified Grashof number
$H_0$	Intensity of magnetic field
$M$	Hartmann number
$N$	Thermal radiation
$Pe$	Peclet number
$Re$	Reynolds number
$Sc$	Schmidt number
$u$	Axial velocity

$B_0$	Uniform magnetic field
$Ec$	Eckert number
$G$	Gravitational force
$Gr$	Grashof number
$K$	Chemical reaction parameter
$m$	Taperedness parameter
$p$	Pressure
$q$	Radiative heat flux
$S$	Porous shape parameter
$t$	Time

### 3. Mathematical formulation

MHD oscillatory blood flow has been analyzed by taking blood as second order fluid in presence of magnetic field. Blood flow through lumen present in veins and arteries considered as porous channel in tapered wavy shape due to diseased nervous system and its geometry is shown in Fig. 1.

The following assumptions are made:

- Blood is considered as a suspension of micro elements in plasma and optically thick viscoelastic fluid.
- Blood is assumed to be uniformly dense in the portion like arteries taken for discussion.
- The inner most layer lumen in the blood vessel can be taken as porous structure due to the deposit of substances like lipids and cholesterol.
- Magnetic force is assumed in orthogonal to the blood channel.
- Rosseland approximations applied with radiative heat transfer term  $q_r$ , so that heat flux approximated as first degree in temperature  $T^*$ .

The equations of asymmetric walls ( $H_1, H_2$ ) are given by

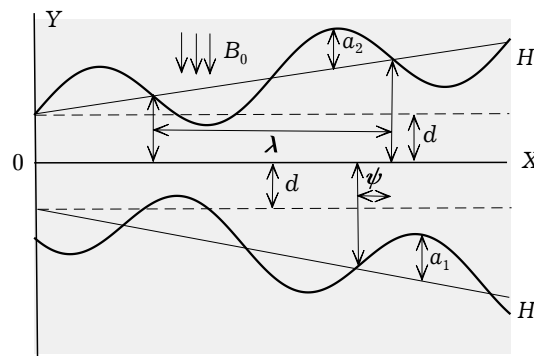


Fig. 1. Geometry of the asymmetric tapered channel.

$$H_1 = -d - mx^* - a_1 \sin \left[ \frac{2\pi}{\lambda}(x^*) + \psi \right],$$

$$H_2 = d + mx^* + a_2 \sin \left[ \frac{2\pi}{\lambda}(x^*) \right],$$

where the non-uniform parameter  $m$  represents taperedness of the channel,  $\lambda$  is the wave length and  $\psi$  is the phase angle of wavy channel.

The parameters  $a_1$ ,  $a_2$ ,  $d$  and  $\psi$  of the channel geometry are subject to the constraint [18]

$$a_1^2 + a_2^2 + 2a_1a_2 \cos(\psi) \leq (2d)^2.$$

#### 4. Governing equations

Governing equations of the blood flow are given by [6]

Momentum equation:

$$\frac{\partial u^*}{\partial t^*} = -\frac{1}{\rho} \frac{\partial p^*}{\partial x^*} + \nu \frac{\partial^2 u^*}{\partial y^{*2}} + \beta_0 \frac{\partial^3 u^*}{\partial y^{*2} \partial t^*} - \frac{\nu u^*}{k^*} - \frac{\sigma_e B_0^2 u^*}{\rho} + g\beta_1(T^* - T_0^*) + g\beta_2(C^* - C_0^*); \quad (1)$$

Energy equation:

$$\frac{\partial T^*}{\partial t^*} = \frac{k}{\rho C_p} \frac{\partial^2 T^*}{\partial y^{*2}} - \frac{1}{\rho C_p} \frac{\partial q^*}{\partial y^*} + \frac{\nu}{\rho C_p} \left( \frac{\partial u^*}{\partial y^*} \right)^2. \quad (2)$$

Using Rosseland approximation [19], the radiative transfer term  $q^*$  may be expressed as

$$q^* = -\frac{4\sigma^*}{3\chi} \frac{\partial T^{4*}}{\partial y^*}. \quad (3)$$

Substituting the equation (3) in (2), the energy equation becomes

$$\frac{\partial T^*}{\partial t^*} = \frac{k}{\rho C_p} \frac{\partial^2 T^*}{\partial y^{*2}} + \frac{16\sigma^* T_0^{*3}}{3\rho C_p \chi} \frac{\partial^2 T^*}{\partial y^{*2}}. \quad (4)$$

Concentration equation:

$$\frac{\partial C^*}{\partial t^*} = D \frac{\partial^2 C^*}{\partial y^{*2}} - K_r^*(C^* - C_0^*), \quad (5)$$

where the term containing  $D$  represents mass diffusion and  $K_r^*$  term represents the chemical reaction.

The corresponding boundary conditions (BCs) are given by

$$\text{when } y^* = h_1, \quad u^* = 0, \quad T^* = T_0^*, \quad C^* = C_0^*;$$

$$\text{when } y^* = h_2, \quad u^* = 0, \quad T^* = T_0^* + (T_1^* - T_0^*)e^{i\omega t}, \quad C^* = C_0^* + (C_1^* - C_0^*)e^{i\omega t}.$$

Introducing non-dimensional variables:

$$\bar{x} = \frac{x^*}{\lambda}, \quad \bar{y} = \frac{y^*}{d}, \quad \bar{t} = \frac{t^* U_0}{d}, \quad \bar{u} = \frac{u^*}{U_0}, \quad \text{Re} = \frac{U_0 d}{\nu}, \quad h_1 = \frac{H_1}{d}, \quad h_2 = \frac{H_2}{d},$$

$$\text{Gr} = \frac{g\beta d^2 (T^* - T_0^*)}{\nu U_0}, \quad \text{Gc} = \frac{g\beta_C d^2 (C_1^* - C_0^*)}{\nu U_0}, \quad M^2 = \frac{\sigma B_0^2 d^2}{\rho \nu},$$

$$\theta = \frac{(T^* - T_0^*)}{(T_1^* - T_0^*)}, \quad \phi = \frac{(C^* - C_0^*)}{(C_1^* - C_0^*)}, \quad \bar{p} = \frac{d^2 p}{\rho \nu U_0}, \quad \beta = \frac{\beta_0 U_0}{\nu d}, \quad N = \frac{4\alpha^2 d^2}{k},$$

$$\text{Pe} = \frac{\rho C_p U_0 d}{k}, \quad \text{Ec} = \frac{\rho C_p U_0^2}{k(T_1^* - T_0^*)}, \quad K = \frac{d K_r^*}{U_0}, \quad \bar{\omega} = \frac{\omega^* d}{U_0}. \quad (6)$$

Applying transformation (6) in (1), (4) and (5), the governing equations in dimensionless form are obtained after omitting the bars, as

Momentum equation:

$$\text{Re} \frac{\partial u}{\partial t} = -\frac{\partial p}{\partial x} + \frac{\partial^2 u}{\partial y^2} + \beta \frac{\partial^3 u}{\partial y^2 \partial t} - (s^2 + M^2)u + \text{Gr} \theta + \text{Gc} \phi;$$

Energy equation:

$$\text{Pe} \frac{\partial \theta}{\partial t} = (1 + N) \frac{\partial^2 \theta}{\partial y^2} + \text{Ec} \left( \frac{du}{dy} \right)^2;$$

Concentration equation:

$$\frac{\partial \phi}{\partial t} = \frac{1}{\text{Sc}} \frac{\partial^2 \phi}{\partial y^2} - K \phi. \quad (7)$$

The BCs in non-dimensional form become,

$$\begin{aligned} y = h_1, \quad u = 0, \quad \theta = 0, \quad \phi = 0, \\ y = h_2, \quad u = 0, \quad \theta = e^{i\omega t}, \quad \phi = e^{i\omega t}. \end{aligned}$$

## 5. Method of solution

Taking pressure gradient in the following form, the flow becomes oscillatory type,

$$-\frac{\partial p}{\partial x} = \lambda e^{i\omega t}.$$

For oscillatory flow, solution of periodic nature can be taken as

$$\begin{aligned} u(y, t) &= u_0(y) e^{i\omega t}, \\ \theta(y, t) &= \theta_0(y) e^{i\omega t}, \\ \phi(y, t) &= \phi_0(y) e^{i\omega t}. \end{aligned}$$

Solving equation (7), subject to the BCs, concentration distribution obtained as,

$$\phi(u, t) = \frac{\sinh m_1(y - h_1)}{\sinh m_1(h_2 - h_1)} e^{i\omega t}.$$

By homotopy perturbation method, solving the following momentum equation and energy equation,

$$u_0'' - P^2 u_0 = \frac{\lambda - \text{Gr} \theta_0 - \text{Gc} \phi_0}{1 + i\omega \beta'},$$

$$(1 + N)\theta_0'' - i\omega \text{Pe} \theta_0 + \text{Pr Ec} \left( \frac{du_0}{dy} \right)^2 = 0.$$

Subject to the BCs:

$$\begin{aligned} y = h_1, \quad u_0 = 0, \quad \theta_0 = \phi_0 = 0, \\ y = h_2, \quad u_0 = 1, \quad \theta_1 = \phi_0 = 1. \end{aligned}$$

The solutions representing flow profiles are obtained as

$$\begin{aligned} u(y, t) = (u_0 + u_1) = \left[ (A_0 e^{Py} + B_0 e^{-Py}) + \frac{1}{1 + i\omega \beta'} \left( -\frac{\lambda}{P^2} - \frac{\text{Gc} \sinh m_1(y - h_1)}{\sinh(m_1 \overline{h_2 - h_1})(m_1^2 - P^2)} \right) \right. \\ \left. + (A_1 e^{Py} + B_1 e^{-Py}) - \frac{\text{Gr}}{1 + i\omega \beta'} \frac{\theta_0}{Q_1^2 - P^2} \right] e^{i\omega t}, \end{aligned}$$

$$\begin{aligned} \theta(y, t) = (\theta_0 + \theta_1) = \left[ (C_0 e^{Q_1 y} + D_0 e^{-Q_1 y}) + (C_1 e^{Q_1 y} + D_1 e^{-Q_1 y}) \right. \\ \left. - \left( \frac{\text{Pr Ec}}{1 + N} \right) \left( \frac{P^2 (e^{2Py} A_0^2 + e^{-2Py} B_0^2)}{4P^2 - Q_1^2} - \frac{1}{2} \frac{A_2^2}{Q_1^2} - \frac{A_2^2 \cosh(2ml(h_1 - y))}{2Q_1^2 - 8m_1^2} \right) \right] e^{i\omega t} \end{aligned}$$

$$\begin{aligned}
& - A_0 A_2 P \left( \frac{e^{Py-m_1(h_1-y)}}{(P+m_1)^2 - Q_1^2} - \frac{e^{Py+m_1(h_1-y)}}{Q_1^2 - (P-m_1)^2} \right) \\
& + A_2 B_0 P \left( \frac{e^{m_1(h_1-y)-Py}}{(P+m_1)^2 - Q_1^2} - \frac{e^{Py-m_1(h_1-y)}}{Q_1^2 - (P-m_1)^2} \right) \left( \frac{2m_1(h_1-y)}{2Q_1^2 - 8m_1^2} + \frac{2A_0 B_0 P^2}{Q_1^2} \right) \Big] e^{i\omega t}, \\
\phi(y, t) &= \frac{\sinh m_1(y-h_1)}{\sinh m_1(h_2-h_1)} e^{i\omega t}.
\end{aligned}$$

All the constants appearing in the above solutions are given by

$$\begin{aligned}
m_1 &= \sqrt{\frac{i\omega + K}{Sc}}, \\
A_0 &= \frac{1}{2(1+i\omega\beta) \sinh P(h_1-h_2)} \left[ \frac{\lambda}{P^2} e^{P(h_2-2h_1)} - \left( \frac{\lambda}{P^2} + \frac{Gr}{m_1^2 - P^2} \right) e^{-Ph_1} \right] + \frac{\lambda}{P^2(1+i\omega\beta')} e^{-Ph_1}, \\
B_0 &= \frac{1}{1+i\omega\beta'} \left[ \left( \frac{\lambda}{P^2} + \frac{Gr}{m_1^2 - P^2} \right) e^{Ph_1} - \frac{\lambda}{P^2} e^{Ph_2} \right] \frac{1}{2 \sinh P(h_1-h_2)}, \\
C_0 &= \frac{1}{e^{Q_1 h_2} - e^{2Q_1 h_1 - Q_1 h_2}} = \frac{e^{-Q_1 h_1}}{e^{Q_1(h_2-h_1)} - e^{-Q_1(h_2-h_1)}}, \\
D_0 &= \frac{-e^{Q_1 h_1}}{e^{Q_1(h_2-h_1)} - e^{-Q_1(h_2-h_1)}}, \\
A_1 &= \frac{Gr e^{-Ph_1}}{2 \sinh P(h_2-h_1)} \frac{1}{(1+i\omega\beta')(Q_1^2 - P^2)}, \\
B_1 &= \frac{-Gr e^{Ph_1}}{(1+i\omega\beta')(Q_1^2 - P^2)} \frac{1}{2 \sinh P(h_2-h_1)}, \\
C_1 &= \frac{C_3 e^{-Q_1 h_2} - C_2 e^{2Q_1(h_1-h_2)}}{1 - e^{2Q_1(h_1-h_2)}}, \\
D_1 &= \frac{C_2 e^{Q_1(h_1+2h_2)} - C_3 e^{Q_1(2h_1+h_2)}}{e^{2Q_1 h_2} - e^{2Q_1 h_1}}, \\
A_2 &= \frac{m_1 Gc}{(1+i\omega\beta')(m_1^2 - P^2)} \frac{1}{\sinh[m_1(h_2-h_1)]}, \\
C_2 &= \frac{P^2 (e^{2Ph_1} A_0^2 + e^{-2Ph_1} B_0^2)}{4P^2 - Q_1^2} - \frac{A_2^2}{2Q_1^2 - 8m_1^2} - \frac{1}{2} \frac{A_2^2}{Q_1^2} \\
& - A_0 A_2 P \left( \frac{e^{Ph_1}}{(P+m_1)^2 - Q_1^2} - \frac{e^{Ph_1}}{Q_1^2 - (P-m_1)^2} \right) \\
& - A_2 B_0 P \left( \frac{e^{-Ph_1}}{(P+m_1)^2 - Q_1^2} - \frac{e^{-Ph_1}}{Q_1^2 - (P-m_1)^2} \right) + \frac{2A_0 B_0 P^2}{Q_1^2}, \\
C_3 &= \frac{P^2 (e^{2Ph_2} A_0^2 + e^{-2Ph_2} B_0^2)}{4P^2 - Q_1^2} - \frac{1}{2} \frac{A_2^2}{Q_1^2} - \frac{A_2^2 \cosh(2m_1(h_1-h_2))}{2Q_1^2 - 8m_1^2} + \frac{2A_0 B_0 P^2}{Q_1^2} \\
& + A_0 A_2 P \left( \frac{e^{Ph_2+m_1(h_1-h_2)}}{Q_1^2 - (P-m_1)^2} - \frac{e^{Ph_2-m_1(h_1-h_2)}}{(P+m_1)^2 - Q_1^2} \right) \\
& - A_2 B_0 P \left( \frac{e^{-Ph_2-m_1(h_1-h_2)}}{Q_1^2 - (P-m_1)^2} - \frac{e^{m_1(h_1-h_2)-Ph_2}}{(P+m_1)^2 - Q_1^2} \right), \\
P^2 &= \frac{s^2 + M^2 + i\omega Re}{1 + i\omega\beta'}, \\
Q_1^2 &= \frac{i\omega Pe}{1 + N}.
\end{aligned}$$

## 6. Results and discussion

In this problem on the analysis of MHD oscillatory blood flow, the impact of different parameters on flow profiles are presented.

### 6.1. Velocity profiles

Velocity profiles drawn for various flow parameters with  $t = 0.1$ ,  $m = 0.5$ ,  $Re = 0.5$ ,  $K = 1$ ,  $Gc = 0.5$  and  $Ge = 1$ .

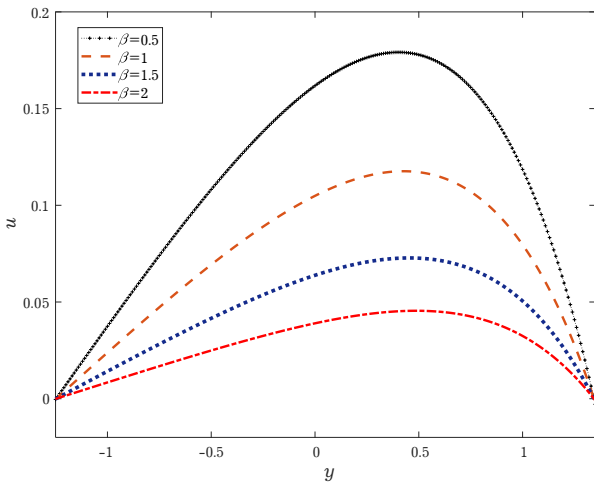


**Fig. 2.** Visco elastic influence on velocity for  $Pr = 0.7$ ,  $Pe = 0.3$ ,  $H = 1$ ,  $S = 1$ ,  $N = 0.5$ ,  $\lambda = 1$ .

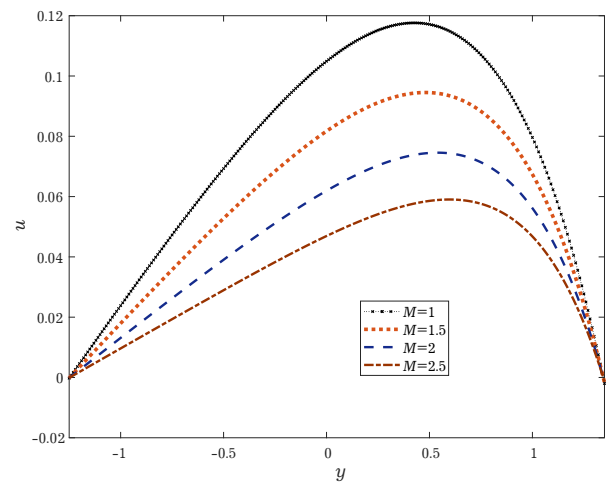


**Fig. 3.** Hartmann number influence on velocity for  $Pr = 0.7$ ,  $Re = 0.5$ ,  $Pe = 0.3$ ,  $\beta = 1$ ,  $S = 1$ ,  $N = 0.5$ ,  $\lambda = 1$ .

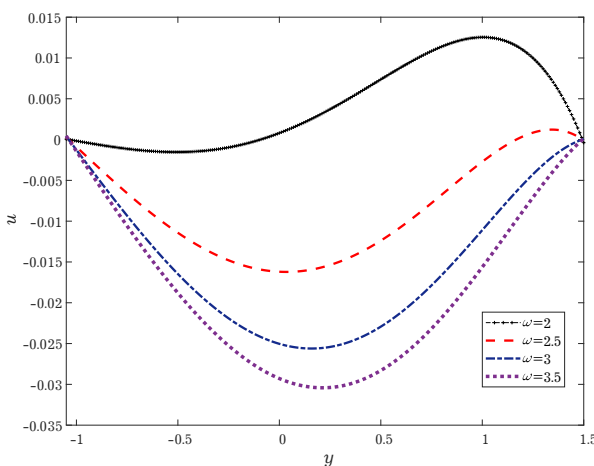


**Fig. 4.** Oscillation influence on velocity for  $t = 0.1$ ,  $m = 0.5$ .

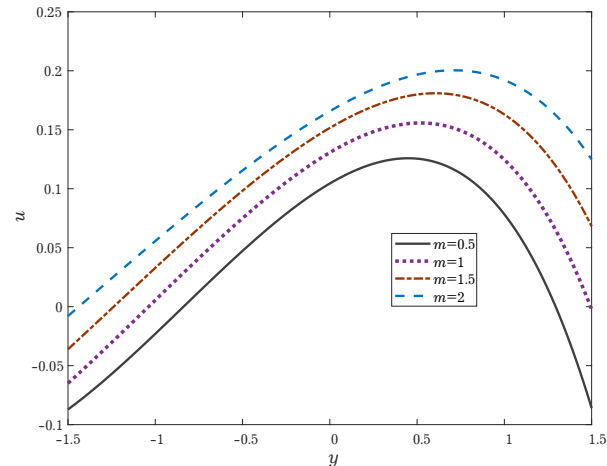


**Fig. 5.** Non uniform channel parameter influence on velocity for  $\beta = 1$ ,  $Pr = 0.7$ ,  $Pe = 0.3$ ,  $H = 1$ ,  $S = 1$ ,  $N = 0.5$ ,  $\lambda = 1$ .

Results on velocity distribution due to the impact of Hartmann number ( $M$ ), frequency of oscillation ( $\omega$ ), viscoelastic parameter ( $\beta$ ), non-uniform parameter ( $m$ ), Grashoff number ( $Gr$ ) and radiation ( $N$ ) are discussed in Figs. 2–7. The impact of viscoelastic parameter ( $\beta$ ) on velocity is shown in Fig. 2. With the increase in viscoelastic parameter ( $\beta$ ) velocity is observed to be decreasing and taking maximum near middle of the channel. Variation in velocity is lesser for values of viscoelastic parameter ( $\beta$ ) around 2 compared to the variations for  $\beta < 1.5$ .

When the parameter Hartmann number ( $M$ ) increases, velocity is decreasing and verifying Hartmann’s result on Lorentz force, as seen in Fig. 3. From Fig. 4, as the parameter frequency of oscillation

( $\omega$ ) increases velocity decreases and observed that magnitude of velocity is greater for  $\omega = 2$ . As  $\omega$  increases from 2.5 to 3.5, velocity diminishes rapidly taking minimum value at the middle of the channel.

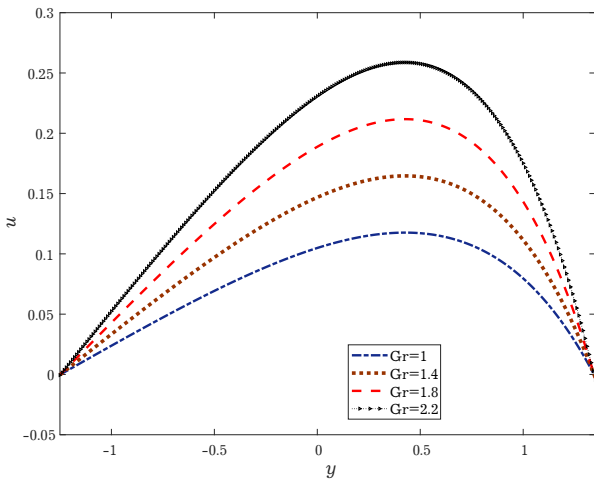


**Fig. 6.** Grashoff number influence on velocity for  $Pr = 0.7, K = 1, Pe = 0.3, H = 1, \beta = 1, S = 1, N = 0.5, \lambda = 1$ .

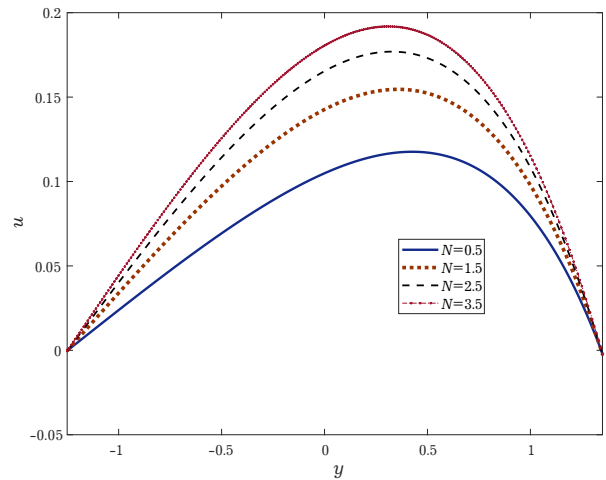


**Fig. 7.** Radiation influence on velocity for  $Pr = 0.7, K = 1, Pe = 0.3, H = 1, S = 1, \beta = 1, \lambda = 1$ .

With the increase in non-uniform parameter ( $m$ ), velocity distribution is increasing, reaching maximum near the right boundary  $y = h_1$ , as seen from Fig. 5. From Figs. 6, 7, the velocity distribution is observed to be increasing and taking maximum value at  $y = 0.4$  when the parameter Grashoff number ( $Gr$ ) (or) radiation ( $N$ ) increases.

### 6.2. Temperature profiles

Temperature profiles drawn for various flow parameters with  $Pe = 0.3, t = 0.1, m = 0.2$  and  $N = 2$ .

Graphs plotted in Figs. 8–12 are prepared to analyze the response of temperature due to the impact of parameters associated with energy profile. As Fig. 8 shows the influence of non-uniform parameter ( $m$ ) on temperature as non-uniform parameter ( $m$ ) increases, temperature diminishes due to increase in taperedness of the channel. From Fig. 9, as frequency of oscillation ( $\omega$ ) increases temperature is diminishing and not showing much variation in temperature.

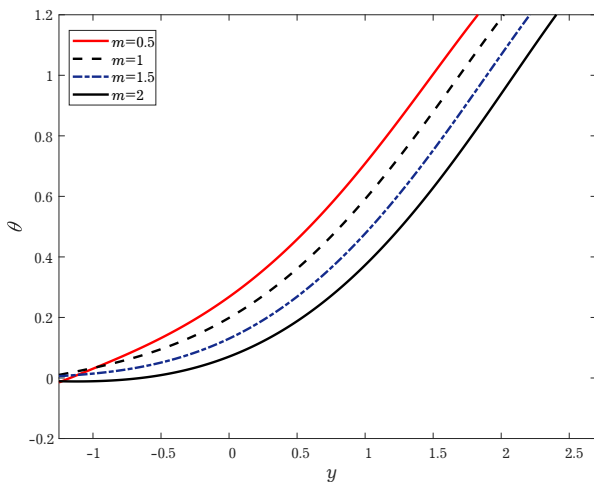


**Fig. 8.** Non uniform channel parameter influence on temperature for  $Pr = 0.7, Re = 0.5, K = 1, \beta = 0.5, Gc = 0.5, Gr = 1, S = 1, H = 1, d = 1, \omega = 1, \lambda = 1$ .

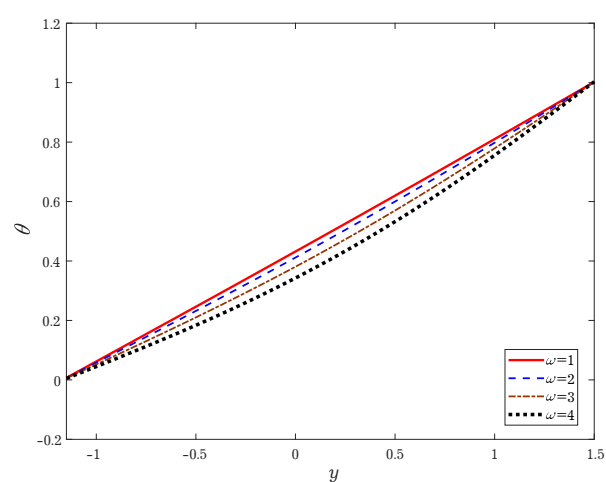


**Fig. 9.** Frequency of oscillation influence on temperature for  $Pr = 0.7, Re = 0.5, K = 1, \beta = 0.5, Gc = 0.5, Gr = 1, S = 1, H = 1, d = 1, \lambda = 1$ .



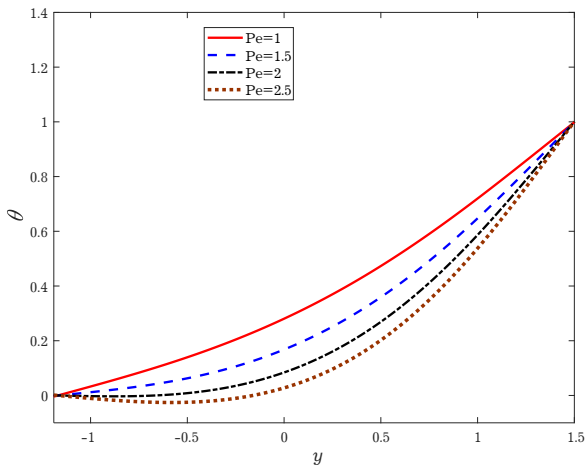


**Fig. 10.** Peclet number influence on temperature for  $Pr = 0.7, Re = 0.5, K = 1, \beta = 0.5, Gc = 0.5, Gr = 1, S = 1, H = 1, d = 1, \lambda = 1.$

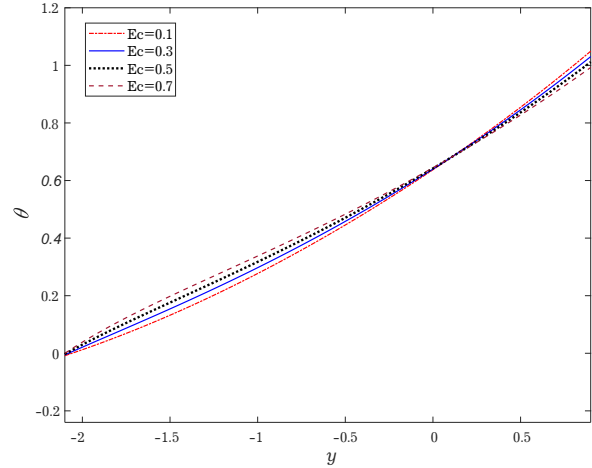


**Fig. 11.** Eckert number influence on temperature for  $Pr = 0.7, Re = 0.5, K = 1, \beta = 0.5, Gc = 0.5, Gr = 1, S = 1, H = 1, d = 1, \omega = 1, \lambda = 1.$

With the increase in Peclet number (Pe), temperature distribution is observed to be decreasing with reduced variation in temperature for  $Pe > 2$  as shown in Fig. 10. In Fig. 11, as Eckert number (Ec) increases, temperature is increasing for  $-2 < y < 0$  and then temperature decreases for  $0 < y < 0.9$ . As seen from Fig. 12, temperature increases due to increase in radiation (N). Temperature distribution reaches maximum as radiation increases to the value 2.

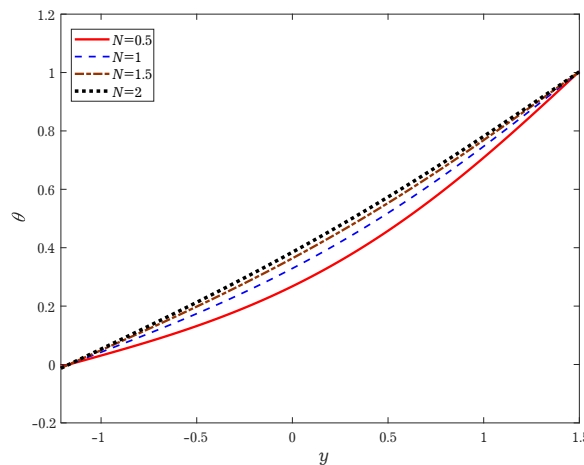


**Fig. 12.** Radiation influence on temperature for  $Pr = 0.7, Re = 0.5, K = 1, \beta = 0.5, Gc = 0.5, Gr = 1, S = 1, H = 1, d = 1, \omega = 1, t = 0.1, \lambda = 1.$

### 6.3. Concentration profiles

Concentration profiles drawn for various flow parameters with  $t = 0.1$  and  $m = 0.5$ .

In Figs. 13, 14, concentration diminishes with the raise in ( $K$ ) (or) in frequency of oscillation ( $\omega$ ). From Fig. 15, as Schmidt number increases from  $Sc = 1$  to  $Sc = 4$  concentration increases, with less variations for  $Sc > 2$ . From Fig. 16, as Schmidt number increases from  $Sc = 0.1$  to  $Sc = 1.2$ , it is observed that concentration increases. For  $Sc > 0.2$ , concentration shooting up with large variation. For smaller values of ( $Sc$ ) around 0.1, concentration is constant in the region between left boundary  $y = h_2$  to middle of the channel. In the other half of the channel concentration increases exponentially.

**Table 1.** Sherwood number values obtained by Venkateshwaralu [20] and in the present work.

	Venkateshwaralu	Present work
Schmidt number (Sc)	Sherwood number (Sh)	Sherwood number (Sh)
0.1	1.1780	1.1912
0.2	1.0927	1.1071
0.3	1.0613	1.0589
0.4	1.0464	1.0415

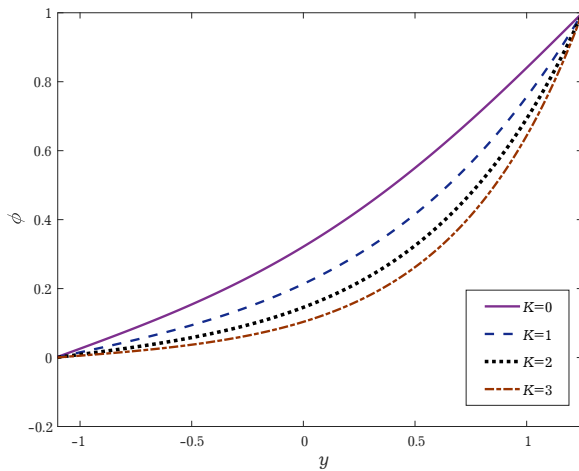


**Fig. 13.** Chemical reaction influence on concentration for  $\omega = 1$ ,  $Sc = 1$ .

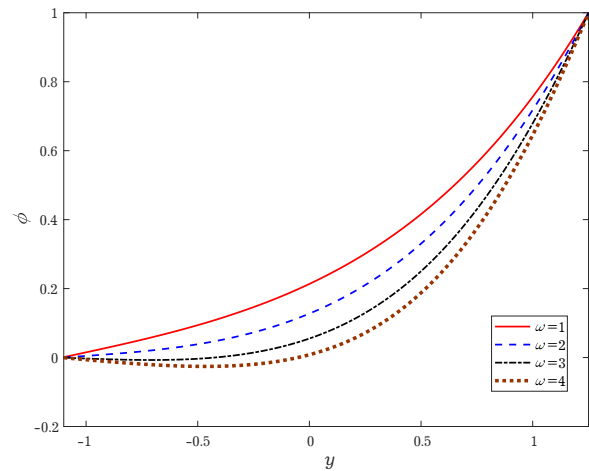


**Fig. 14.** Oscillation Influence on Concentration for  $K = 1$ ,  $Sc = 1$ .

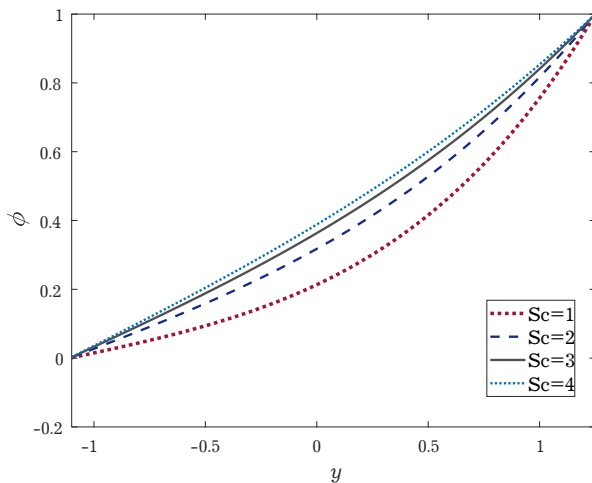


**Fig. 15.** Schmidt number influence on concentration for  $\omega = 1$ ,  $K = 1$ ,  $Sc = 1$ .

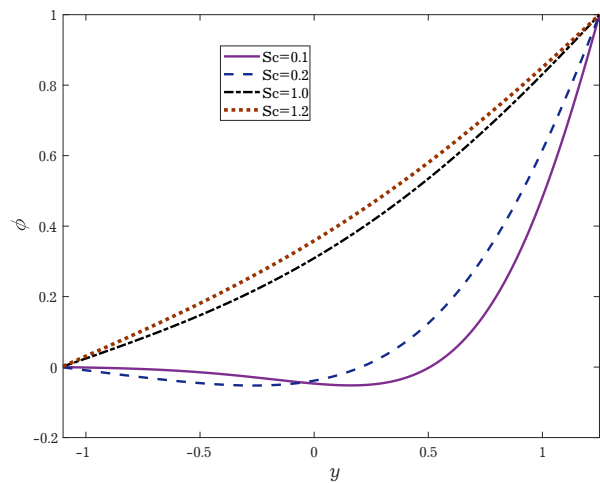


**Fig. 16.** Schmidt number influence on concentration for  $\omega = 1$ ,  $K = 1$ ,  $Sc = 1$ .

## 7. Conclusion

The following are the important findings derived out of this study on MHD oscillatory blood flow, analyzing influence of various parameters on velocity ( $u$ ), temperature ( $\theta$ ) and concentration ( $\phi$ ) profiles. Velocity ( $u$ ) distribution enhances with increase in Grashoff number ( $Gr$ ), non-uniform parameter ( $m$ ) and radiation ( $N$ ). Temperature ( $\theta$ ) distribution reduces with the increase in  $m$ ,  $\omega$  and  $Pe$ . Increase in Eckert number ( $Ec$ ) impacting very little variation in temperature ( $\theta$ ). Raise in radiation ( $N$ ), increases the temperature ( $\theta$ ) distribution. The impact of ( $K$ ) on ( $\phi$ ), reduces ( $\phi$ ) with minimum variation for larger values of  $K$ . Frequency of oscillation  $\omega$  reduces the concentration ( $\phi$ ) profiles. For smaller values of Schmidt number ( $Sc$ ), concentration ( $\phi$ ) shows variation of larger magnitude and as Schmidt number ( $Sc$ ) takes larger values, variations in  $\phi$  are lesser. In the present work, taking limit as  $a, b, m \rightarrow 0$ ,  $Ec \rightarrow 0$  results are coinciding with work done by Venkateshwaralu [20].

- 
- [1] Ramachandra Rao A., Deshikacharan K. S. MHD oscillatory flow of blood through channels of variable cross section. *International Journal of Engineering Sciences*. **24** (10), 1615–1628 (1986).
  - [2] Ogulu A., Abbey T. M. Simulation of heat transfer on an oscillatory blood flow in an indented porous artery. *International Communications in Heat and Mass Transfer*. **32** (7), 983–989 (2005).

- [3] Mustapha N., Amina N., Chakravarty S., Kumar Mandal P. Unsteady magnetohydrodynamic blood flow through irregular multi-stenosed arteries. *Computers in Biology and Medicine*. **39** (10), 896–906 (2009).
- [4] Hatami M., Hatami J., Ganji D. D. Computer simulation of MHD blood conveying gold nanoparticles as a third grade non-Newtonian nano fluid in a hollow porous vessel. *Computer Methods and Programs in Biomedicine*. **113** (2), 632–641 (2014).
- [5] Shit G. C., Majee S. Pulsatile flow of blood and heat transfer with variable viscosity under magnetic and vibration environment. *Journal of Magnetism and Magnetic Materials*. **388**, 106–115 (2015).
- [6] Misra J. C., Adhikary S. D. MHD oscillatory channel flow, heat and mass transfer in a physiological fluid in presence of chemical reaction. *Alexandria Engineering Journal*. **55** (1), 287–297 (2016).
- [7] Bhatti M. M., Ali Abbas M. Simultaneous effects of slip and MHD on peristaltic blood flow of Jeffrey fluid model through a porous Medium. *Alexandria Engineering Journal*. **55** (2), 1017–1023 (2016).
- [8] Akbarzadeh P. Pulsatile magneto-hydrodynamic blood flowthrough porous blood vessels using a third gradenon-Newtonian fluids model. *Computer Methods and Programs in Biomedicine*. **126**, 3–19 (2016).
- [9] Sinha A., Misra J. C., Shit G. C. Effect of heat transfer on unsteady MHD flow of blood in a permeable vessel in the presence of non-uniform heat source. *Alexandria Engineering Journal*. **55** (3), 2023–2033 (2016).
- [10] Mirza I. A., Abdulhameed M., Vieru D., Shafi S. Transient electro-magneto-hydrodynamic two-phase blood flow and thermal transport through a capillary vessel. *Computer Methods and Programs in Biomedicine*. **137**, 149–166 (2016).
- [11] Hsiao K.-L. Micropolarfluid flow with MHD and viscous dissipation effects towards a stretching sheet with multimedia feature. *International Journal of Heat and Mass Transfer*. **112**, 983–990 (2017).
- [12] Majee S., Shit G. C. Numerical investigation of MHD flow of blood and heat transfer in a stenosed arterial. *Journal of Magnetism and Magnetic Materials*. **424**, 137–147 (2017).
- [13] Ali D., Sen S. Permeability and fluid flow-induced wall shear stress of bone tissue scaffolds: Computational fluid dynamic analysis using Newtonian and non-Newtonian blood flow models. *Computers in Biology and Medicine*. **99**, 201–208 (2018).
- [14] Kafle J., Gaire H. P., Pokhrel P. R., Kattel P. Analysis of blood flow through curved artery with mild stenosis. *Mathematical Modeling and Computing*. **9** (2), 217–225 (2022).
- [15] Sasikumar J., Gayathri R., Govindarajan A. Heat and Mass Transfer Effects on MHD Oscillatory flow of a Couple Stress fluid in an Asymmetric Tapered channel. *IOP Conference Series: Materials Science and Engineering*. **402** (1), 012167 (2018).
- [16] Vijayalakshmi T., Senthamarai R. Study of two species prey–predator model in imprecise environment with harvesting scenario. *Mathematical Modeling and Computing*. **9** (2), 385–398 (2022).
- [17] Suganya G., Senthamarai R. Mathematical modeling and analysis of Phytoplankton–Zooplankton–Nano-particle dynamics. *Mathematical Modeling and Computing*. **9** (2), 333–341 (2022).
- [18] Kothandapani M., Srinivas S. Peristaltic transport of a Jeffrey fluid under the effect of magnetic field in an asymmetric channel. *International Journal of Non-Linear Mechanics*. **43** (9), 915–924 (2008).
- [19] Predikis C., Raptis A. Heat transfer of a micropolar fluid by the presence of radiation. *Heat Mass Transfer*. **31**, 381–382 (1996).
- [20] Venkateshwaralu B., Satya Narayana P. V., Devika B. Effects of chemical reaction and heat source on MHD oscillatory flow of a viscoelastic fluid in a vertical porous channel. *International Journal of Applied and Computational Mathematics*. **3** (1), 937–952 (2017).

## Вплив хімічних реакцій та в'язкої дисипації на МГД коливний кровотік у конічному асиметричному каналі

Сасікумар Дж., Сентхамарай Р.

*Факультет математики, Інженерно-технологічний коледж,  
Інститут науки і технологій SRM, Каттанкулатур-603 203,  
Район Ченгалпатту, Тамілнаду, Індія*

МГД в'язкий коливний кровотік через просвіт артерій і варикозних вен спонукає до вивчення кровотоку в уражених кровоносних судинах і венах. Кровотік у неупорядкованій нервовій системі, як-от варикозне розширення вен та інших мікроартерій у дихальній системі, моделюється геометрично у формі звужених вигнутих стінок різного поперечного перерізу, що є новим підходом до цієї проблеми та має перевагу порівняно з іншими геометричними формами каналу. Кров вважають в'язкопружною й оптично густою рідиною, що протікає через пористу структуру. Магнітна сила розглядається в нормальному напрямку до нервової системи. Проаналізовано вплив в'язкої дисипації та хімічних реакцій на кровотік.

**Ключові слова:** *кровотік, оптично густа рідина, хімічна реакція та в'язка дисипація.*